

See discussions, stats, and author profiles for this publication at: <https://www.researchgate.net/publication/20891299>

Hydrodynamic study of flexibility in immunoglobulin IgG1 using Brownian dynamics and the Monte Carlo simulations of a simple model

ARTICLE *in* BIOPOLYMERS · FEBRUARY 1990

Impact Factor: 2.39 · DOI: 10.1002/bip.360300507 · Source: PubMed

CITATIONS

14

READS

4

3 AUTHORS, INCLUDING:



F. Guillermo Díaz Baños

University of Murcia

47 PUBLICATIONS 472 CITATIONS

SEE PROFILE



José García de la Torre

University of Murcia

217 PUBLICATIONS 6,099 CITATIONS

SEE PROFILE

Hydrodynamic Study of Flexibility in Immunoglobulin IgG1 Using Brownian Dynamics and the Monte Carlo Simulations of a Simple Model

F. G. DÍAZ, A. INIESTA, and J. GARCÍA DE LA TORRE*

Departamento de Química Física, Facultad de Ciencias Químicas y Matemáticas,
Universidad de Murcia, Espinardo, 30100 Murcia, Spain

SYNOPSIS

A simple bead model is proposed for the antibody molecule immunoglobulin IgG1. The partial flexibility of the hinge is represented by a quadratic potential associated to the angles between arms. Conformational and hydrodynamic properties are calculated using Monte Carlo (rigid-body) and Brownian dynamics simulations. Comparison of experimental and calculated values for some overall properties allows the assignment of dimensions and other model parameters. The Brownian dynamics technique is used next to simulate a rotational correlation function that is comparable with the decay of fluorescence emission anisotropy. This is done with varying flexibility at the hinge. The longest relaxation time shows a threefold decrease when going from the rigid Y-shaped conformation to the completely flexible case. The calculations are in good agreement with the decay times observed for IgG1. A flexibility analysis of the latter indicates that a variability of $\pm 55^\circ$ (standard deviation) in the angle between the Fab arms.

INTRODUCTION

In some of the most important biological macromolecules, flexibility is localized in a few regions that connect some practically rigid segments. Thus, such macromolecules are able to do one specific physiological function or a variety of different duties.¹ The first (and one of the most interesting) macromolecules to which the segmental flexibility concept was applied were antibodies.^{2,3} These have been described as adaptor molecules linking antigen and effector, being able to function in a wide variety of situations. It is accepted that antibodies have a remarkable flexibility in the joint of the arms (Fab fragments) and Fc that form the typical Y-shape first proposed by Valentine and Green⁴ and this has been confirmed in the most recent studies.^{5,6} In another way some other studies (for instance, tridimensional crystal structure studies) have shown the

possibility of some flexible regions in the subunits^{5,7} but fluorescence depolarization measurements indicate that this flexibility is less important than the one localized at the joint.^{2,8-11}

Hydrodynamic properties like sedimentation or diffusion coefficients depend essentially on the overall conformation of the macromolecules and are not very sensitive to segmental flexibility, which is better detected in the decay of fluorescence polarization anisotropy. A rigorous prediction of anisotropy decay for segmentally flexible particles can be done simulating on a computer the Brownian dynamics of a hydrodynamic bead model. In this paper, we propose a model for IgG1 that has four beads representing the three subunits and the hinge region. Literature data of translational diffusion, radius of gyration, and intrinsic viscosity are used to estimate plausible values for the dimensions of the model by comparison of calculated or simulated results with experimental data. Then the rotational and segmental motion that determine the anisotropy decay are simulated using the Brownian dynamic technique. The aspect and rate of the decay are analyzed in terms of the degree of flexibility in the hinge.

© 1990 John Wiley & Sons, Inc.
CCC 0006-3525/90/5-60547-08 \$04.00

Biopolymers, Vol. 30, 547-554 (1990)

* To whom correspondence should be addressed.

Our study is focused on human IgG1 because it is a very typical immunoglobulin and there are various experimental results we can compare in the theoretical work, but there is no restriction in applying the same treatment to different kinds of antibodies.

MODEL AND METHODS

Our first purpose is to build a model with a small number of beads that reproduces the experimental data taken from the literature.¹² The simplest way to model a Y-shaped structure is by considering three spheres to describe the arms and another small sphere in the joint of the model, as shown in Figure 1. In this model flexibility is considered by assuming variability in the angles between arms (α_1 , α_2 , and α_3 in Figure 1). To describe this flexibility we have assigned a quadratic potential to each angle

$$V_i(\alpha_{0,i}) = \frac{1}{2}k_e(\alpha_i - \alpha_{0,i})^2, \quad i = 1, 2, 3 \quad (1)$$

where k_e is the elasticity constant and $\alpha_{0,i}$ are the equilibrium angles. Instead of k_e , it is now convenient to use the Q parameter defined by

$$Q = \frac{k_e}{2k_b T} \quad (2)$$

where $k_b T$ is the Boltzmann factor. Thus, we are assuming that the flexibility is the same for the three angles. Although this may not be true in the real molecule, its influence in our semiquantitative conclusions will not be important.

The connectors between subunits are rather stiff Hookean springs with a potential

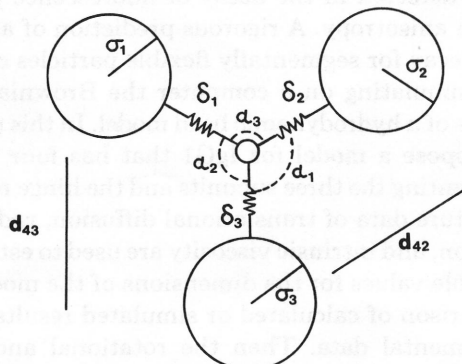


Figure 1. Geometry of the four-sphere model for IgG1 according to Ref. 12. Values for the parameters are shown in Table I.

$$U_i(b_i) = \frac{1}{2\delta_i^2} (b_i - b_{0,i})^2 \quad (3)$$

where δ_i is a stretching constant and $b_{0,i}$ the equilibrium length between the central sphere and the i subunit.

The last contribution to the potential accounts for steric interaction between arms. It is evident that the arms in the IgG molecule cannot penetrate each other. In the model, this interaction can be conveniently represented by a Lennard-Jones expression. For noncontiguous spheres we have

$$J_{ij}(r_{ij}) = 4\epsilon_{ij}[(\sigma_{ij}/r_{ij})^{12} - (\sigma_{ij}/r_{ij})^6] \quad (4)$$

where σ_{ij} is the zero-potential distance and ϵ_{ij} is the well depth.

The forces for each subunit are then described by

$$\mathbf{F}_1 = \nabla_{\mathbf{r}_1}(V_2 + V_3 + U_1 + J_{12} + J_{13}) \quad (5a)$$

$$\mathbf{F}_2 = \nabla_{\mathbf{r}_2}(V_1 + V_3 + U_2 + J_{12} + J_{23}) \quad (5b)$$

$$\mathbf{F}_3 = \nabla_{\mathbf{r}_3}(V_1 + V_2 + U_3 + J_{13} + J_{23}) \quad (5c)$$

$$\mathbf{F}_4 = -\sum_{i=1}^3 \mathbf{F}_i \quad (5d)$$

Brownian Dynamics

Having specified the geometric and energetic parameters of the model, the Brownian dynamics simulation technique can be applied to the study of macromolecular properties. The simplest and most used algorithm for Brownian dynamics simulation is that proposed ten years ago by Ermak and McCammon.¹³⁻¹⁶ In this algorithm, if \mathbf{r}_i^0 is the position vector of the i th frictional element of a macromolecular model that has N elements (in our study $N = 4$), then the position vector \mathbf{r}_i after a time step Δt is given by

$$\begin{aligned} \mathbf{r}_i &= \mathbf{r}_i^0 + \frac{\Delta t}{kT} \sum_j \mathbf{D}_{ij}^0 \cdot \mathbf{F}_j^0 \\ &\quad + \Delta t \sum_j \left(\frac{\partial \mathbf{D}_{ij}}{\partial \mathbf{r}_j} \right)^0 + \mathbf{R}_i(\Delta t) \end{aligned} \quad (6)$$

where \mathbf{F}_j^0 is the force on the j th element and \mathbf{R}_i is a Gaussianly distributed random vector with zero mean and covariance $2\mathbf{D}_{ij}\Delta t$. \mathbf{D}_{ij}^0 is the ij block of the diffusion tensor that includes the individual mobilities of the beads as well as the hydrodynamic interaction between them. In the simulations we are

going to use the expression for \mathbf{D}_{ij} proposed by Rotne–Prager–Yamakawa^{17,18} for spheres of the same size and corrected later by García de la Torre and Bloomfield¹⁹ for different spheres. The superscript 0 denotes the conformation before the time step. Using the vectors \mathbf{r} , \mathbf{R} , and \mathbf{F} , and $3N$ components (three for each bead) and the $3N \times 3N$ diffusion tensor \mathbf{D} , Eq. (6) can be written in a more compact manner:

$$\begin{aligned} \mathbf{r} = \mathbf{r}^0 + (kT)^{-1} \Delta t \mathbf{D}^0 \cdot \mathbf{F}^0 \\ + \Delta t (\nabla_{\mathbf{r}} \cdot \mathbf{D})^0 + \mathbf{R}(\Delta t) \end{aligned} \quad (7)$$

As an alternative to Eq. (7), we have recently proposed the use of a second-order algorithm in which every step is a combination of two first-order steps.²⁰ A first-order estimate of the position after a time step Δt , now denoted as \mathbf{r}' , is obtained from Eq. (7). Then the time step is repeated, but using the mean of the quantities \mathbf{D} , $\mathbf{D} \cdot \mathbf{F}$, and $\nabla_{\mathbf{r}} \mathbf{D}$ at positions \mathbf{r}^0 and \mathbf{r}' . Thus we have

$$\begin{aligned} \mathbf{r} = \mathbf{r}^0 + (kT)^{-1} \Delta t \left\{ \frac{1}{2} (\mathbf{D}^0 \cdot \mathbf{F}^0 + \mathbf{D}' \cdot \mathbf{F}') \right. \\ \left. + \frac{1}{2} ((\nabla_{\mathbf{r}} \cdot \mathbf{D})^0 + (\nabla_{\mathbf{r}} \cdot \mathbf{D}')) \right\} + \mathbf{R} \end{aligned} \quad (8)$$

where

$$\langle \mathbf{R}(\Delta t) \mathbf{R}(\Delta t) \rangle = 2 \left(\frac{1}{2} (\mathbf{D}^0 + \mathbf{D}') \right) \Delta t \quad (9)$$

Brownian dynamics can be used to obtain the translational diffusion coefficient, D_t from the well-known equation of Einstein

$$\langle [\mathbf{r}(t) - \mathbf{r}(0)]^2 \rangle = 2 D_t t \quad (10)$$

where t is time and \mathbf{r} is the position vector of the particle.

The radius of gyration of a multisubunit structure can be obtained using²¹

$$R_G^2 = \sum f_i \langle c_i^2 + R_{G_i}^2 \rangle \quad (11)$$

where f_i is the volume fraction, c_i is the distance to the center of mass, and R_i is the radius of gyration, all of them of the i th element.

The internal motions of the arms of the immunoglobulin model can be described by the correlation function for the second Legendre polynomial in the cosine of the angle $\zeta(t)$ subtended by two orientations of the arm separated by time t :

$$\langle P_2(t) \rangle = \langle P_2[\cos \zeta(t)] \rangle \quad (12)$$

More details about Brownian dynamics simulation of the simple rigid and semiflexible models, and the procedures to evaluate averages and correlation functions from the simulated trajectories, are described elsewhere.^{13–16}

Rigid Body Approximation Using a Monte Carlo Simulation

The hydrodynamics of segmentally flexible macromolecules can be approached from the well-developed theory for rigid particles using the so-called rigid body approximation^{22–26} in which properties are evaluated as averages of values obtained for the possible conformations, which are regarded as instantaneously rigid.²⁷

We have used a Monte Carlo simulation procedure of the Metropolis type. Starting from some set of angles α'_i , we generate a new state using the usual procedure. A new orientation is obtained from the preceding one by adding small random changes to the α'_i angles, calculating the new values α_i from the preceding one as $\alpha_i = \alpha'_i + \Delta\alpha_i$. $\Delta\alpha_i$ are random numbers with uniform distribution in $(-\Delta\alpha, \Delta\alpha)$. For a set of angles the potential energy V is

$$V = \sum_{i=1}^3 V_i \quad (13)$$

where V_i is given by Eq. (1). If $V \leq V'$, where V' is the potential for the previous state, the new state is accepted. If $V > V'$, a random number u uniformly distributed in $(0, 1)$ is generated. If $u \leq \exp[(V' - V)/kT]$, the new state is accepted; otherwise, it is rejected and the previous one is counted again. We consider rigid connectors between spheres and situations with overlapping spheres are forbidden.

In the rigid-body treatment we generate a high number of possible conformations. For everyone we calculate R_G , using Eq. 12, and D_t and $[\eta]$ with the rigid body theory.²⁷ The final results are the averages of the instantaneous values over all the generated conformations. The procedure can be carried out for various Q 's corresponding to different degrees of flexibility.

RESULTS AND DISCUSSION

Model Parameters

We assume that the primary parameters for fitting initially the structure could be the volumes of the subunits. In this sense we have tried to simplify the

model of Kilar et al.¹² using spheres with the same volumes as the ellipsoids and cylinders that they used. The equilibrium lengths of the connectors between the central sphere and the i -subunits $b_{0,i}$ that we are going to use in Eq. 3 are identical for the two Fab subunits (from the joint to the center of the cylinder); for the Fc fragment, due to the presence of the hole, we have used two thirds of the distance between the joint and the center of the cylinder in the Kilar's model. The parameters of our model are shown in Table I and Figure 1.

Inspired by the Y shape, we take in our model equilibrium angles between arms $\alpha_{0,i} = 120^\circ$ for $i = 1, 2, 3$ (see Table I). The last parameters we need are the stretching constant δ for the Hookean potential [Eq. (3)] and the zero-potential distance σ_{ij} , for the Lennard-Jones potential [Eq. (4)]. We can consider that the spring connecting subunits is practically rigid when $\delta = 0.1$.¹³ On the other hand, σ_{ij} is the sum of the radii of the noncontiguous spheres i, j ($\sigma_{ij} = \sigma_i + \sigma_j$; see Table I).

It should be remarked that the parameters assigned to the subunits may not agree with a variety of existing (and sometimes contradictory) data for their individual properties. The spherical shape for the subunits can indeed be an even more drastic assumption. As commented above and discussed in detail later on, these oversimplifications, which are needed to build workable model of IgG, do not essentially influence the conclusions of our work.

Conformational Statistics

The purpose of the statistical calculations is to check our Brownian dynamics simulation and to determine the model parameters, including the flexibility constants of Brownian dynamics has been used to gen-

erate. Conformations of the model have been determined by Brownian dynamics using the following simulation parameters: $\Delta t = 0.0025$ (in normalized units that correspond to 1.23 ns); 5×10^4 steps divided in 5 subtrajectories (for obtaining statistical error); γ varies from $Q = 50$ (practically rigid) to $Q = 0$ (flexible).

Carrying out some calculations for the distribution of connector lengths (results not shown), we have confirmed first that $\delta = 0.1$ is a good value for describing quasirigid connectors in this model. On the other hand, in Figure 2 we show, as expected, that with $Q = 0$ in α_1 , α_2 , and α_3 (totally flexible case, without excluded volume, see below) we have an uniform distribution in the cosine of any angle, while with $Q = 50$ we find the expected peak around $\cos \alpha \cong -0.5$ ($\alpha = 120^\circ$). Figure 2 also shows that the range defining the semiflexible model is $0 < Q \lesssim 1-4$ and for a value of $Q = 50$ the distribution is flat, as it should be in the completely flexible case.

It is interesting to have a flexible model that avoids overlapping of spheres (excluded volume). As commented above, we can use the Lennard-Jones potential [Eq. (4)] to describe this kind of interaction. We have studied (as shown in Figure 3) the influence of the well depth parameter (ϵ) in the distribution of distances, finding that for $\epsilon < 0.5$ the probability of overlapping configurations grows quickly and if $\epsilon > 0.5$ the distribution is affected in an important way (one unexpected peak appears). These are the reasons for our choice of $\epsilon = 0.5$.

Overall Properties

After setting plausible values for the model parameters and before the lengthy simulation of internal dynamics, we obtained three properties that depend

Table I Model Parameters

i^a	1	2	3	4
σ_i (Radius; nm)	2.44 (0.42) ^b	2.44 (0.42)	2.56 (0.44)	0.44 (0.075)
V_i (Volume; nm ³)	60.8	60.8	70.3	0.36
R_{Gi} (Radius of gyration; nm)	1.89	1.89	1.98	0.34
i^a	1	2	3	
$b_{0,i}$ (Connector lengths; nm)	6.10 (1.04)	6.10 (1.04)	5.87 (1)	
i^a	1	2	3	
$\alpha_{0,i}$ (Equilibrium angles)	120°	120°	120°	

^a See Figure 1.

^b Data in brackets are in normalized units (referred to 3–4 connector length, b_{03}).

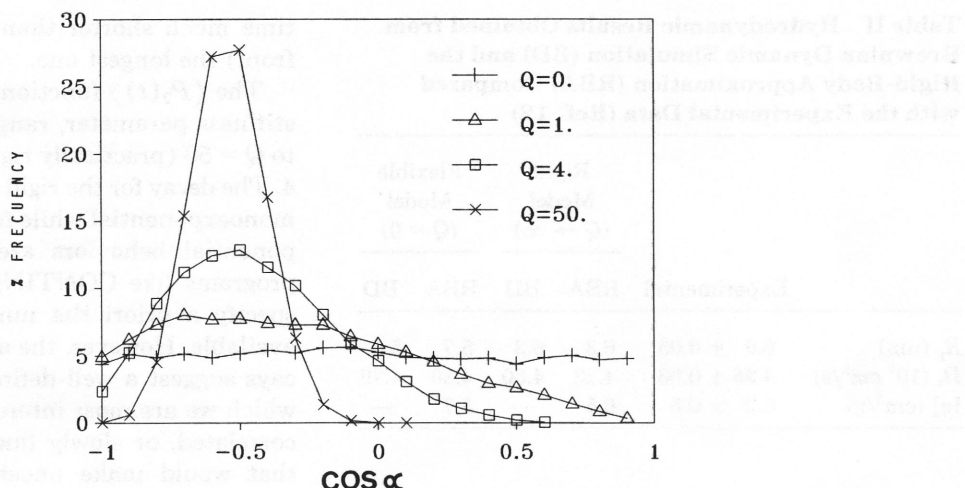


Figure 2. Distribution for the cosine of any of the α angles (see Figure 1) obtained from Brownian dynamics simulation without excluded volume for different values of the flexibility constant Q .

essentially on the overall conformation of the molecule: the radius of gyration, the translational diffusion coefficient, and the intrinsic viscosity.

To do so, we used two methods: the rigid body approximation and Brownian dynamics. Calculations with the first method have been made with typically 2500 conformations (divided in 5 subsamples) and 45° for $\Delta\alpha$. In the second one the same parameters as for statistics were used (see above). In Table II these results are shown along with the experimental ones.¹² We can see that differences between both theoretical treatments are negligible in the rigid limit. Differences in the flexible limit are

due to the small but finite probability of overlapping between beads that is allowed by the Lennard-Jones potential and that is not considered in the rigid-body approximation. These differences are more noticeable for the radius of gyration (12%), but we think they are not relevant for the general conclusions of this work.

As expected, the radius of gyration, the viscosity, and the diffusion coefficient do not depend strongly on flexibility (the maximum variation is approximately 20%). That is the reason why these magnitudes are not most appropriate for a definitive study of the flexibility of the model. Anyhow, they

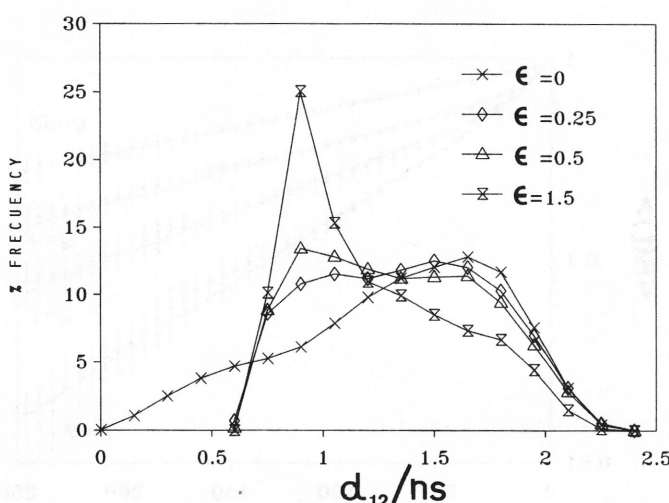


Figure 3. Distribution of the connector lengths (distance 1-2, 1-3, and 1-4) obtained from Brownian dynamics simulation for different values of the Lennard-Jones parameter ϵ .

Table II Hydrodynamic Results Obtained from Brownian Dynamic Simulation (BD) and the Rigid-Body Approximation (RBA) Compared with the Experimental Data (Ref. 12)

	Rigid Model ($Q \rightarrow \infty$)		Flexible Model ($Q = 0$)	
Experimental	RBA	BD	RBA	BD
R_g (nm)	6.0 ± 0.05	6.3	6.3	5.7
D_t (10^7 cm 2 /s)	4.25 ± 0.06	4.23	4.30	4.50
$[\eta]$ (cm 3 /g)	6.2 ± 0.5	6.5	—	5.7

are valid enough to affirm that this model can give a plausible description of the hydrodynamic behavior of IgG1, because experimental data are within their range of error between the theoretical limiting values in all cases.

Internal Motions and Fluorescence Anisotropy Decay

From a long trajectory of 5×10^5 steps of $\Delta t = 0.25 \times 10^{-3}$ (reduced units), we evaluated the decay of the correlation function $\langle P_2(t) \rangle$ defined in Eq. (12). In the decay of fluorescence emission anisotropy, the decay is proportional to $\langle P_2(t) \rangle$ (and has therefore the same relaxation times) if either the absorption or the emission dipole are along the arm axis. Otherwise, there would be an additional component in the decay, corresponding roughly to a torsion of the arm around its axis, but with a relaxation

time much shorter than (and therefore separable from) the longest one.

The $\langle P_2(t) \rangle$ functions for various values of the stiffness parameter, ranging from $Q = 0$ (flexible) to $Q = 50$ (practically rigid) are displayed in Figure 4. The decay for the rigid Y-shaped particle is nearly monoexponential while for intermediate Q multiexponential behaviors are observed. Sophisticated programs like CONTIN, which do not require to specify a priori the number of components, are available. However, the aspect of our simulated decays suggest a well-defined long-time behavior, in which we are most interested, or otherwise display correlated, or slowly fluctuating, statistical errors that would make uncertain the applicability of CONTIN. Note that in all cases the decay curves were adequately represented by two exponential. A nonlinear least-squares fitting to an expression of the form

$$\langle P_2(t) \rangle = Ae^{-t/\tau_1} + (1 - A)e^{-t/\tau_2} \quad (14)$$

gives the parameters listed in Table III. The most remarkable result is the longest relaxation time τ_1 , which ranges from 64 ns for $Q = 0$ to 202 ns for very high Q . Given the A values listed in Table III, the average relaxation time used sometimes by experimentalists, $\langle \tau \rangle = A\tau_1 + (1 - A)\tau_2$, is practically equal to τ_1 .

Reidler et al.¹¹ reported $\langle \tau \rangle$ values of 84 and 109 ns for two IgG1 molecules. Their experimental results are well bracketed by our calculations in the two limits of flexibility, and are closer to the flexible limit than to the rigid one. These authors stated

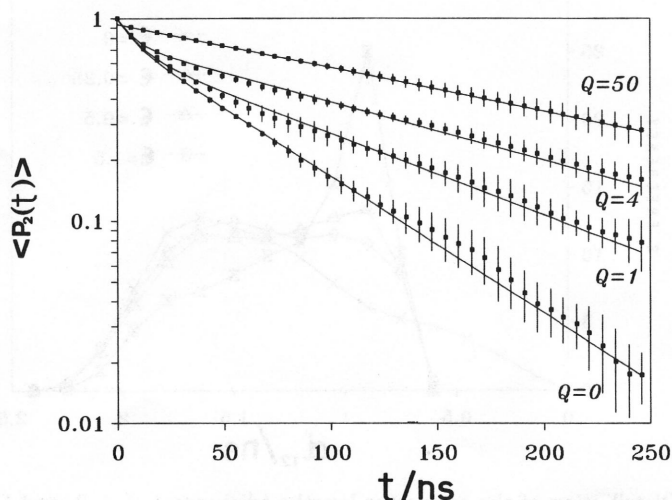


Figure 4. Decay of the $\langle P_2(t) \rangle$ function for arm reorientation for models with varying flexibility.

Table III Amplitudes and Relaxation Times of the $\langle P_2(t) \rangle$ Decay for Varying Flexibility Parameter

<i>Q</i>				
	50	4	1	0
<i>A</i>	0.935	0.746	0.681	0.780
τ_1 (ns)	202	151	109	64
τ_2 (ns)	—	8	11	9

that "calculations of the rotational correlation time of rigid and partially flexible Y-shaped molecules, using recently developed theories²⁷ were needed to determine the angular range of motion of the Fab arms." We can now answer that need. Their experimental data give roughly an average of $Q \approx 0.6$. In Figure 2 we see that for a higher value of the parameter, $Q = 1$, the probability density of $\cos \alpha$ is nearly featureless and rather flat. If the distribution of angle α were a Gaussian centered at $\alpha_0 = 120^\circ$, from Eqs. (1) and (2) we find that $Q = 0.6$ corresponds to a standard deviation of about 55° . Thus, although IgG1 is not completely flexible, the α angle between the Fab arms can easily span from a T shape to a conformation with nearly touching Fab arms.

The above analysis of IgG1 flexibility is qualitatively correct but the resulting estimates may be influenced by the choice of numerical parameters. These are in turn determined by the experimental values of overall properties of IgG1 taken from the literature. In this regard, systematic data for the individual fragments are needed. With such data a more accurate parameterization of the model could be done, which would result in a more quantitative description of IgG1 flexibility. Anyhow, we think that the present estimate is rather informative from the point of view of immunoglobulin function.

A result that must be rather insensitive to the choice of geometric parameters is the ratio of the longest relaxation times in the two limits, $\tau_1(Q \rightarrow \infty)/\tau_1(Q = 0)$. Our results indicate that this ratio is about 3. In other words the long-time decay of anisotropy in a completely flexible IgG should be about three times faster than for a rigid Y-shaped molecule. Stryer, Oi et al.²⁸⁻³⁰ have measured the decay for a variety of monoclonal and genetically engineered antibodies, finding that the longest and shortest relaxation times differ by a factor of roughly 2, which is in accord with our theoretical prediction. Factors other than flexibility may of course determine the observed variability. Indeed, some part of the differences in relaxation rates could be due to

differences in size and shape in the subunits. As new information on structure and solution properties for a diversity of immunoglobulin G molecules is emerging, we hope that Brownian dynamics simulation like the one carried out in this preliminary work will be helpful in learning about segmental flexibility of antibodies.

This work was supported by grants from the Comisión Interministerial de Ciencia y Tecnología (PB87-0694) and Acciones Integradas Hispano-Británicas. FGD acknowledges a fellowship from the Plan de Formación de Personal Investigador. We are grateful to Dr. S. Harding (University of Nottingham) and Drs. K. Davis and D. Burton (University of Sheffield) for their comments.

REFERENCES

- Richardson, J. S. (1981) *Adv. Protein Chem.* **34**, 168–174.
- Yguerabide, J., Epstein, H. F. & Stryer, L. (1970) *J. Mol. Biol.* **51**, 573–590.
- Yguerabide, J. (1973) *Methods Enzymol.* **26**, 498–579.
- Valentine, R. C. & Green, H. M. (1967) *J. Mol. Biol.* **27**, 615–617.
- Burton, D. R. (1987) in *Molecular Genetics of Immunoglobulin*, Calabi, F., & Neuberger, M. S., Eds., Elsevier Science Publishers B. U. (Biomedical Division), Amsterdam.
- Burton, D. R. (1989) in *Antibodies and Microbial Infection*, Metzger, H., Ed., American Microbiology Society, Washington, DC, in press.
- Huber, R. (1980) *Klin. Wochenschr.* **58**, 1217–1231.
- Lovejoy, C., Holokawa, D. A. & Cathou, R. E. (1977) *Biochemistry* **16**, 3668–3672.
- Chan, L. M. & Cathou, R. E., (1977) *J. Mol. Biol.* **112**, 653–656.
- Hanson, D. C., Yguerabide, J. & Schumaker, V. N., (1981) *Biochemistry* **20**, 6842–6852.
- Reider, J., Oi, V. T., Carlsen, W., Pecht, T., Unomg, T. M., Herzenberg, L. A. & Stryer, L. (1982) *J. Mol. Biol.* **158**, 739–746.
- Kilar, F., Simon, I., Lakatos, S., Vanderviszt, F., Medgyesi, G. A. & Závouchiský, P. (1985) *Eur. J. Biochem.* **147**, 17–25.
- Díaz, F. G., Iniesta, A. & García de la Torre, J. (1987) *J. Chem. Phys.* **87**, 6021–6028.
- Ermak, D. L. & McCammon, J. A. (1979) *J. Chem. Phys.* **69**, 1352–1360.
- Allison, S. A. & McCammon, J. A. (1984) *Biopolymers* **23**, 167–187.
- Díaz, F. G. & García de la Torre, J. (1988) *J. Chem. Phys.* **88**, 7698–7705.
- Rotne, J. & Prage, S. (1969) *J. Chem. Phys.* **50**, 4831–4837.

18. Yamakawa, H. (1970) *J. Chem. Phys.* **53**, 436-443.
19. García de la Torre, J. & Bloomfield, V. A. (1977) *Bio-polymers* **16**, 1747-1763.
20. Iniesta, A. & García de la Torre, J. (1990) *J. Chem. Phys.*, in press.
21. Solvez, J. A., Iniesta, A. & García de la Torre, J. (1988) *Int. J. Biol. Macromol.* **10**, 39-44.
22. Zimm, B. H. (1980) *Macromolecules* **13**, 592-602.
23. Hagerman, P. & Zimm, B. H. (1981) *Biopolymers* **20**, 1481-1502.
24. García de la Torre, J., Jimenez, A. & Freire, J. J. (1982) *Macromolecules* **15**, 148-154.
25. García de la Torre, J., López Martinez, M. C., Tirado, M. M. & Freire, J. J. (1984) *Macromolecules* **17**, 2715-2722.
26. García de la Torre, J. (1989) in *Dynamics Properties of Macromolecular Assemblies*, Harding, S. C. & Rowe, A., Eds., The Royal Society of Chemistry, in press.
27. García de la Torre, J. & Bloomfield, V. A. (1981) *Quart. Rev. Biophys.* **14**, 81-139.
28. Schneider, W. P., Wensel, T. G., Stryer, L. & Oi, V. T. (1988) *Proc. Natl. Acad. Sci. USA* **85**, 2509-2513.
29. Oi, V. T., Vuong, T. M., Hardy, R., Reidler, J., Dangl, J., Herzenberg, L. A. & Stryer, L. (1984) *Nature* **307**, 136-140.
30. Dangl, J. L., Wensel, T. G., Morrison, S. L., Stryer, L., Herzenberg, L. A. & Oi, V. T. (1988) *EMBO J.* **7**, 1989-1994.

Received January 9, 1990

Accepted March 19, 1990